Proceedings of IPACK2007
ASME InterPACK '07
July 8-12, 2007, Vancouver, British Columbia, CANADA

IPACK2007-33554

THERMAL PERFORMANCE MEASUREMENTS OF THERMAL INTERFACE MATERIALS USING THE LASER FLASH METHOD

Vinh Khuu, Michael Osterman, Avram Bar-Cohen, and Michael Pecht
Department of Mechanical Engineering
University of Maryland
College Park, MD

ABSTRACT

Thermal interface materials are used to reduce the interfacial thermal resistance between contacting surfaces inside electronic packages, such as at the die-heat sink or heat spreader-heat sink interfaces. In this study, the change in thermal performance was measured for elastomeric gap pads, gap fillers, and an adhesive throughout reliability tests. Three-layer composite structures were used to simulate loading conditions encountered by thermal interface materials in actual applications. The thermal resistance of the thermal interface material, including contact and bulk resistance, was calculated using the Lee algorithm, an iterative method that uses properties of the single layers and the 3-layer composite structures, measured using the laser flash method. Test samples were subjected to thermal cycling tests, which induced thermomechanical stresses due to the mismatch in the coefficients of thermal expansion of the dissimilar coupon materials. The thermal resistance measurements from the laser flash showed little change or slight improvement in the thermal performance over the course of temperature cycling. Scanning acoustic microscope images revealed delamination in one group of gap pad samples and cracking in the putty samples.

INTRODUCTION

Thermal interface materials (TIMs) play a critical role in the thermal management of electronics by providing a path of low thermal impedance between a heat-generating component, such as a chip and a heat sink. Due to increasing power dissipation levels occurring in a variety of microelectronic applications, minimizing the interfacial thermal resistance between contacting surfaces can be crucial in maintaining component operating temperatures at acceptable levels [1]. In many microprocessor and discrete RF applications, the resistance is 30 to 50% of the total thermal resistance budgets [2]. A wide array of TIM types, such as greases, phase change materials, pads, films, and adhesives are now commercially available. The selection process can be challenging since the overall performance of a TIM depends on many factors including process variables, assembly conditions, bulk material properties, and properties of the interface, which may require characterization to accurately assess the effects on the thermal performance [3].

NOMENCLATURE

R = thermal resistance
k = thermal conductivity
BLT = bond line thickness
α_{CTE} = CTE
τ = shear stress
G = shear modulus
T = temperature
l = length
E = Young's Modulus
A = cross-sectional area
ν = Poisson's ratio
$t_{1/2}$ = half-rise time
L = thickness
α = thermal diffusivity
η_i = square root of the heat diffusion time
H = volumetric specific heat
V = normalized temperature
X = function of H
ω = function of the heat diffusion time ratio
Q = heat pulse function

BACKGROUND

Since thermal resistance most directly reflects the intended function and the thermal performance, it was used to characterize the TIMs in this study. Thermal resistance values reported in this study are the sum of the contact resistances $R_{contact1}$ and $R_{contact2}$ at each interface and the bulk resistance of the TIM:

$$R_{total} = BLT / k_{TIM} + R_{contact1} + R_{contact2} \quad (1)$$

where BLT is the bondline thickness and k_{TIM} is the bulk thermal conductivity of the TIM layer. Many techniques exist to measure the thermal conductivity of TIMs, and the appropriateness of a method can depend on the type of TIM being studied. The laser flash method and the modified hot wire method are transient methods that have relatively fast measurement speeds and can be used to measure various TIM types, such as greases and adhesives. Steady state techniques, such as the guarded heat flow method and the guarded comparative longitudinal heat flow method, are commonly used by TIM vendors. However, the validity of the standards associated with these measurement methods, namely ASTM D5470 [4] and ASTM E1530 [5], has been questioned since reproducibility of vendor data is often difficult to achieve and the test conditions, such as the contact pressures and sample thicknesses, often do not correspond to typical in-use conditions [2]. Deficiencies in the ASTM standards have prompted many researchers to offer modifications or develop new test methods [3,6,7].

Characterizing the in-situ performance of a TIM using test vehicles based on standard packages is another approach that several groups have used to ensure that the loading conditions of the TIM are realistic [8,9]. However, using a test vehicle that is too specific to a single application may cause difficulty in extending the results to packages with different configurations and environmental conditions.

The proper selection of a TIM often requires not only considering the thermal performance, but also the reliability, which is often not characterized by vendors. Previous research on the reliability of TIMs has centered on thermal greases, which are among the most widely used TIM. Gowda et al. [10] studied the effects of filler material, particle size, and distribution on the performance of thermal greases. The effects of filler particle size and modulus of cured gel TIMs on the thermal performance and reliability has been studied [11]. Eveloy et al. [12] measured the effects of creep on pressure sensitive adhesives.

In this study, the thermal performance and reliability of thermal interface materials are examined using the laser flash method and a 3-layer calculation to determine the thermal resistance of TIMs assembled in 3-layer sandwich structures. This approach has been applied by other researchers to the study of thermal greases [13] and solders [14]. Both studies demonstrated the use of scanning acoustic microscopy to assess voiding effects leading to increased thermal resistance over time. Campbell et al. [15] also characterized die attach adhesives using laser flash measurements of 3-layer composite samples. Exploring issues involved in applying the laser flash method to the characterization the thermal performance of TIMS, notably gap pads and fillers, is thus one of the goals of this study.

While reliability problems such as “pump out” and “dry-out” have been reported to occur for thermal greases after prolonged use, the reliability of gap pads and gap fillers has been less studied. The relatively large bondline and inability of gap pads to flow and fill in the microscopic openings in a surface contributes to the low thermal performance compared to greases, gels, and solders. Maguire et al. [16] incorporated gap pad TIMs into their case study of TIMs in high power amplifier designs, while Gwinn and Webb [6] compared the performance of a variety of TIMs including gap pads using published data. The performance over time when subjected to stress was not evaluated in both of these studies. Viswanath et al [17] reported that typical failure mechanisms in thermal pads are increased thermal resistance due to inadequate pressure or loss of contact at one or more surfaces. The extent of degradation and its causes for gap pads and gap fillers has yet to be fully described in the literature and are therefore examined in this study, along with an adhesive for comparison. The change in interfacial contact resistance caused by elevated temperatures is of particular interest in this study since it is hypothesized that delamination could cause degradation in thermal performance for the gap pad, gap fillers, and putties, which are generally regarded as being among the most reliable TIM types. However, increased wetting of the surfaces may also occur, leading to reduced thermal resistance at the interfaces. The primary goal of this study is to determine whether degradation due to temperature cycling occurs in these types of materials and to quantify the change in thermal performance**.**

EXPERIMENTS

Laser flash diffusivity was used to characterize the thermal performance of TIM samples in this study, and additional measurements were performed to obtain mechanical and thermal properties of the coupons and the TIMs to determine the thermal resistance of the TIM samples. The scanning acoustic microscope was also applied to the composite TIM samples to reveal delamination or voiding that could cause a reduction in the performance.

Laser Flash Method

The laser flash method, a technique well-suited for measuring thin, solid, homogeneous test samples, has come into widespread use due to its advantages in terms of measurement speed and sample size. Parker et al. [18] proposed the laser flash method as a means of measuring the thermal diffusivity of a material. Various researchers proposed refinements to more accurately describe the heat transfer occurring during the measurement, including Cowan [19], who

modified the Parker model to account for heat loss in the test sample due to radiation and Clark and Taylor [20], who used similar assumptions as Cowan but considered the heating part of the temperature rise curve. These methods differ fom the Parker method in how the thermal diffusivity is calculated from a measured temperature rise curve.

The laser flash technique involves monitoring the temperature of the back surface of a test sample after a burst of energy is applied to the front surface and the resulting temperature rise propagates through the material. A laser usually supplies the energy burst and the temperature rise curve from the detector, usually an infrared detector, yields the thermal diffusivity of the test sample as well as the specific heat when a reference measurement is also performed. When the thermal diffusivity and specific heat are known, the thermal conductivity can be calculated using the definition of the thermal diffusivity ($\alpha=k/\rho \cdot cp$). In this study, the thermal diffusivity is determined using the Koski procedure, which requires time and temperature ratios of various points along the temperature rise curve [21].

Test Procedure

TIM samples were assembled to achieve a desired bondline thickness or contact pressure and then prepared for the laser flash measurements. Baseline laser flash measurements were then performed prior to temperature cycling and three thermal performance measurements were conducted over the course of the temperature cycling test. Scanning microscope images were taken of the samples after undergoing temperature cycling, and a separate group of samples was measured to assess the morphological changes due to temperature cycling. Twenty samples per type were measured to achieve statistical confidence in the assembly procedure, the laser flash data, and the three-layer calculations. Temperature cycling tests and corresponding thermal performance measurements were conducted in two groups. Figure 1 summarizes the experimental procedure followed in this study with the number of samples shown in parentheses at each step.

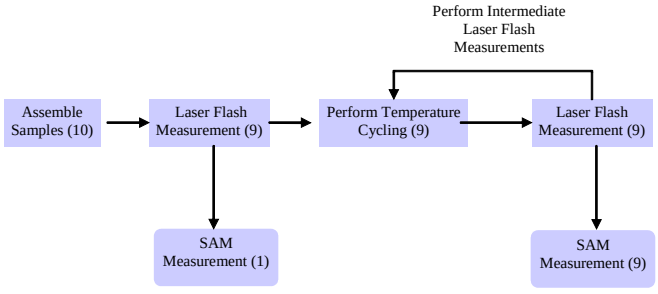

Figure 1: Overview of the Experimental Procedure

TIM Samples and Sample Holder

The test samples examined in this study include thermal gap pads and gap fillers, and an adhesive. Test samples were chosen to represent a range of thermal interface materials and specific samples within a product line were selected based on the thickness constraints of the sample holder. Silicone and non-silicone gap pads with boron nitride filler were evaluated in this study along with a silicone gap filler with boron nitride filler. The gap pads had a thin layer of pressure-sensitive adhesive (PSA) applied to promote adhesion at the interfaces. All materials were suitable for so-called TIM 2 (heat spreader or thermal lid to heat sink) applications although the epoxy adhesive could also be used as a die attachment material (die to substrate). With the exception of the adhesive, all samples were manufactured in pad form. Table 1 summarizes the test samples measured in this study.

Table 1: TIM Test Samples

Label	Putty	Adhesive	Gap filler	Gap Pad A	Gap Pad B
Type	Putty	Epoxy adhesive	Gap filler	Silicone-free gap pad	Silicone gap pad
Material	diamond-filled silicone	filled polymer	filled polymer	filled polymer	filled polymer
Nominal Thickness [mm]	1.5	variable	1	0.5	0.5
***k* [W/m-K] (vendor)**	11	11.4	2.8	0.9	2.4

To simulate realistic loading conditions, laser flash measurements were performed on various TIMs assembled into tri-layer sandwich structures, enabling the test samples to remain undisturbed between measurements performed periodically throughout reliability testing. The test specimens were 3-layer composite samples consisting of the TIM sandwiched between two metal coupons. The coupons were 1 mm thick squares with a side length of 16.4 mm. This size was greater than the typical 8 mm by 8 mm size (used for single layer measurements) to increase the area that the force was applied to the samples when assembled. To set the initial bodnline thickness and facilitate placement in the laser flash system, the layer stack were held in place by aluminum sample holders. Figure 2 shows a sample holder, which was fabricated out of aluminum and required four flat head screws to clamp the plates together.

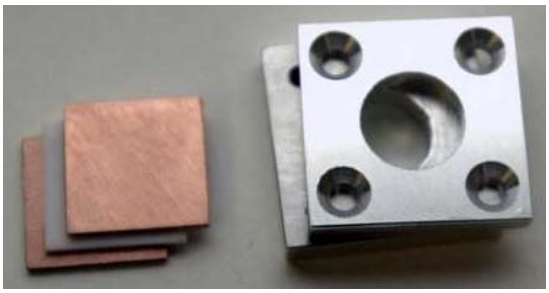

Figure 2: TIM Sample Holder with Three-Layer Composite sample

The coupon materials, oxygen free high conductivity (OFHC) copper and Alloy 42, were selected based on

differences in their coefficients of thermal expansion (CTE) to increase the maximum shear stress. The configuration can be approximated as a bonded assembly of two dissimilar materials with a layer of adhesive subjected to a uniform temperature change. For the adhesive TIM, the maximum shear stress τ occurs at the edges and can be described as follows [22]:

$$\tau_{\max} = \frac{G\Delta T(\alpha_{CTE1} - \alpha_{CTE2})\tanh(Al)}{LA} \qquad (2)$$

$$A^2 = \frac{G}{L}\left(\frac{1-\nu_1}{E_1 A_1} + \frac{1-\nu_2}{E_2 A_2}\right) \qquad (3)$$

where α_{CTE} is the CTE of the coupon, G is the shear modulus of the TIM, ΔT is the temperature difference, l is the TIM layer length, L is the TIM layer thickness, A is the cross-sectional area of the TIM layer, E is the Young's Modulus, and ν is Poisson's ratio. A more detailed analysis is required to determine the stress on the TIM layer when the layer stacks are held in place by a clamping system. Alloy 42 was preferred over other low CTE materials, such as ceramic or silicon, as it is less brittle and prone to cracking when loading is applied. Furthermore, Alloy 42 is less transparent than silicon in the infrared region of the spectrum and does not require a gold coating to reduce the transmittance. The calculated maximum shear stress in a 0.25 mm thick adhesive layer (G = 1.5 GPa) assuming a temperature cycle range of 160 deg C was 9.2 MPa for the copper-Alloy 42 combination (with the same sample geometry used in laser flash measurements). This was less than a 15% difference from 10.8 MPa, the calculated maximum shear stress for the copper-silicon combination. All sample coupons of a given material were fabricated from the same lot to prevent variations in surface roughness between samples from affecting the measurements.

Sample Preparation

The surfaces of the coupons were cleaned with acetone prior to assembling the sandwich structures. Graphite coating was applied to all test sample sandwiches to enhance the absorptivity and emissivity prior to each sequence of laser flash runs. Five coats of graphite were applied in accordance with ASTM E1461 [5] and the laser flash manufacturer directions.

Although the laser flash measurement imposed restrictions on the sample geometry, applying contact force to the TIM allowed loading conditions to more closely match typical usage applications than those used in many bulk conductivity measurement tests. The thermal performance of gap pads and gap fillers, which generally require higher clamping forces for optimal performance compared to thermal greases, is highly dependent on the force loading [16].

Many manufacturers control contact force when characterizing the thermal performance of their thermal interface materials per ASTM D5470, but the stresses in elastomeric materials change over time due to their viscoelastic nature. Since bondline thickness can be more accurately controlled than force, a nominal 25% compression was applied to the gap filler, putty, and gap pad samples during assembly. This thickness value was within the manufacturer's recommended compressed thickness values. The thickness was controlled manually by tightening the samples holder screws and measuring the thickness using a micrometer. Care was taken to ensure that tightening the screws to compress the TIM would result in a uniform thickness and not cause gaps that could have resulted in delamination during assembly.

A 178 μm thick bondline of the epoxy adhesive samples, which were not held under pressure, was maintained using Kapton tape at the corners of the sample, chosen because of its good stability at high temperature. The amount of adhesive dispensed onto the coupon surfaces was controlled manually by the dispenser before the coupons were mated together. The adhesive samples were cured per manufacturer's instructions using a 60 °C prebake for 1 hour and a 150 deg C bake for 0.5 hour. For the adhesive samples, the top and bottom aluminum plates of the sample holder were used to mask the laser beam and radiation from the rear sample and no clamping force was applied by tightening the screws.

Sample thicknesses of the gap pads and fillers were measured with a flat point micrometer, which had an accuracy of 0.025 mm, and values were averaged over five locations on the surface (typically four values near the edges of the beam area and one value in the center).

Laser Flash Measurement

The laser flash method does not provide a direct thermal resistance measurement of the TIM. The TIM thermal resistances is derived from the thermal diffusivity measurement. For this study, an algorithm developed by H.J. Lee [23] and T.Y.R. Lee [24] was used. In the Lee algorithm, the thermal resistance of the TIM layer can be calculated based on properties of the individual layers and the three layer composite. Since interfacial contact resistance cannot be extracted from the three-layer case considered by Lee, the thermal resistance calculated from the algorithm includes both bulk and interfacial contact contributions. Lee's formulation for layered composites relies on the following assumptions:

- 1-D heat flow
- No heat loss from the sample surfaces
- Heat is absorbed uniformly on one side of the sample
- Homogeneous layers
- Constant thermal properties over the temperature range

The half rise time of the temperature response of the composite sample is determined from the apparent diffusivity obtained from the measured data using the following relation:

$$\alpha = \frac{1.388L^2}{\pi \cdot t_{1/2}} \qquad (4)$$

where $t_{1/2}$ = half rise time, L = thickness, and α = thermal diffusivity. The half rise time as well as the single layer properties are then used as inputs into the Lee algorithm. The k^{th} root of the characteristic equation, γ, must then be determined in order to solve for the inverse Laplace of the heat diffusion equations.

$$\cot(\eta_1\gamma)\cot(\eta_2\gamma) + H_{1/3}\eta_{3/1}\cot(\eta_2)\cot(\eta_2\gamma) + H_{2/3}\eta_{3/2}\cot(\eta_3\gamma)\cot(\eta_1\gamma) - 1 = 0 \quad (5)$$

where η_i is the square root of the heat diffusion time through layer i, $\eta_{i/j}$ is the ratio of η_i to η_j and H is volumetric specific heat. The back-side normalized temperature rise of the composite sample can then be calculated based on the algorithm inputs.

$$V = 1 + 2\sum_{k=1}^{\infty} \frac{(\omega_1 X_1 + \omega_1 X_1 + \omega_1 X_1 + \omega_4 X_4)\cdot Q(\gamma_k, \eta_3, t)}{\omega_1 X_1 \cos(\omega_1\gamma) + \omega_2 X_2 \cos(\omega_{12}\gamma) + \omega_3 X_3 \cos(\omega_3\gamma) + \omega_4 X_4 \cos(\omega_4\gamma)} \quad (6)$$

where the X_i terms are functions of H, the ω terms are functions of η_{ij}, and Q is a function of the heat pulse. The diffusivity of the TIM layer is iterated until the normalized temperature using the three-layer composite solution at the half rise time converges to 0.5. The thermal conductivity can then be determined for the converged diffusivity value from the definition of thermal diffusivity.

The density of the TIM layer was calculated by measuring the mass of the sample and the coupons and assuming that the TIM covered the entire face of the coupon (neglecting the material squeezed out when compressed). Furthermore, the vendor value of TIM layer specific heat was used in the thermal resistance calculation for all samples except for the adhesive samples, which required DSC measurement to be performed. Vendor values of thermal diffusivity were determined from specific heat and vendor thermal conductivity values. Measured values for specific heat and thermal diffusivity were used for the coupon layers, as summarized in Table 2, and assumed to be the same among all samples.

Table 2: Copper and Alloy 42 Properties

Material	Property	α (cm^2/s)	c_p (J/gK)	ρ (g/cm^3)	CTE (ppm/°C)
Alloy 42	Vendor/ Handbook	0.026	0.5	8.11	4-6
	Measured	0.041	0.44	8.22	3.2
Copper	Vendor/ Handbook	1.16	0.385	8.94	15
	Measured	1.17	0.4	8.9	14.7

The Lee algorithm [23, 24] requires specific heat values of the individual layers of the composite sample. Due to the difficulty in applying the graphite coating to single layer polymer TIMs, differential scanning calorimetry (DSC) was used for determining the specific heat in samples where vendor data was not provided. DSC is a thermoanalytical technique in which the difference in the amount of heat required to increase the temperature of a sample and reference are measured as a function of temperature. It is generally a more accurate technique for measuring specific heat than the laser flash method as there is no variability in heat pulses between successive runs, and no dependence on coating material or sample surface properties [25].

All laser flash measurements were performed at room temperature. Although it can be shown that the value of the TIM layer thermal resistance is not dependent on which side faces the laser [23], all laser flash measurements were conducted with the copper side facing the laser beam to avoid variation due to the coupon surface finishes. Five flashes were imposed per measurement as this was recommended by the manufacturer. A 50% optical filter, the highest transmittance available for this instrument, was used in the measurements to attenuate the beam power. In preliminary trials the Cowan [19], Clark & Taylor [20], and Parker [18] methods were compared. In most cases little difference was found between the Cowan and Clark & Taylor methods. However, in some instances, the Taylor method could not be used perhaps because of the high signal to noise ratio required. The Parker method often yielded poor fits with the experimental data due to the assumption of no heat loss during the cool down phase. Because of these considerations and for consistency, the Cowan method was used to determine the thermal diffusivity on all the samples. It is to be noted that the Cowan method generally led to lower values of thermal conductivity as compared to values derived from the Parker and Clark/Taylor methods. The Lee algorithm was used to calculate the TIM resistances values presented in this paper.

Room Temperature Observations

Although examining the behavior of TIM samples subjected to temperature cycling was the main objective of this study, separate trials were also performed to characterize the behavior of the samples over time at room temperature. Understanding the room temperature behavior was necessary as some samples could have degraded during room temperature storage. Table 3 summarizes the change in thermal performance over time when stored at room temperature prior to being temperature cycled. Measurements were performed of three samples per type. The time after assembly refers to the time after the TIM was compressed between the sample holder plates and the screws were tightened.

Table 3: TIM Layer Thermal Resistance at Room Temperature

Material	Time after cure/assembly				
	10 minutes	1 hour	1 day	10 days	30 days
Putty	94 ± 7 mm^2K/W	93 ± 7 mm^2K/W	93 ± 6 mm^2K/W	92 ± 7 mm^2K/W	91 ± 7 mm^2K/W
Adhesive	133 ± 21 mm^2K/W	116 ± 7. mm^2K/W	109 ± 12 mm^2K/W	97 ± 6 mm^2K/W	89 ± 5 mm^2K/W
Gap filler	126 ± 18 mm^2K/W	127 ± 15 mm^2K/W	126 ± 15 mm^2K/W	127 ± 13 mm^2K/W	123 ± 14 mm^2K/W
Gap pad A	223 ± 25 mm^2K/W	220 ± 9 mm^2K/W	224 ± 20 mm^2K/W	220 ± 10 mm^2K/W	214 ± 21 mm^2K/W
Gap pad B	74 ± 5 mm^2K/W	75 ± 7 mm^2K/W	72 ± 6 mm^2K/W	69 ± 7 mm^2K/W	61 ± 3 mm^2K/W

After being subjected to a 1 hour prebake at 60 °C and a 0.5 hour bake at 150 °C, the epoxy adhesive showed a 33% reduction in resistance after storage for 1 day at room temperature, reaching a thermal resistance of 89 mm^2K/W. Gap pad B showed the greatest decrease in resistance (18%). Material flow and other relaxation processes, as well as handling (vibration/shock) could have improved the contact between the TIM and coupons after assembly. Storage of the samples over time could have led to a reduction in silicone content in the TIM layer by means of outgassing or extraction, which could have contributed to the observed resistance decreases at room temperature.

Temperature Cycle Testing

Since electronic hardware may experience temperature excursions due to environment or operation, temperature cycle tests were deemed appropriate for this study. Temperature cycling induced thermomechanical stresses in the TIM layer, simulating the loads experienced by TIMs during typical usage. In the absence of a standard method for reliability testing of TIMs, the temperature range was chosen to be -40 to 125 °C, with one cycle lasting for one hour (10 degree per minute ramp rate, fifteen minute dwell at the low and high temperatures). This temperature profile was based on a measurement standard used for surface mount solder attachments [26]. The selected test temperatures were within the normal operating temperature limits of the TIMs specified by their manufacturers.

TEMPERATURE CYCLE RESULTS

For the temperature cycle tests, nine samples of each TIM type were prepared. Measurements were taken prior to temperature cycling, after 255 cycles, 510 cycles, and 760 cycles. The results are summarized in Table 4. Each thermal resistance value is given as a mean value and the standard deviation associated with each of the nine samples (one value per sample is based on an average of five flashes). The resistance change at the end of the temperature cycling tests (relative to the baseline resistance) is also provided.

Table 4: Calculated TIM Thermal Resistance Based on Laser Flash Measurements

	Thermal resistance (mm^2K/W)				
	Putty	Adhesive	Gap filler	Gap pad A	Gap pad B
Predicted (vendor)	101	22	271	633	213
Baseline	80 ± 5	69 ± 7	125 ± 11	253 ± 42	69 ± 7
255 cycles	73 ± 5	61 ± 5	123 ± 12	267 ± 50	52 ± 9
510 cycles	73 ± 6	63 ± 5	124 ± 12	265 ± 51	52 ± 9
760 cycles	67 ± 5	67 ± 6	124 ± 11	269 ± 53	52 ± 9
change after 760 cycles	-13 (-16%)	-2 (-3%)	-1 (-1%)	+16 (+6%)	-17 (-25%)

As shown in Table 5, with the exception of Gap Pad A, a reduction of TIM thermal resistance was observed. It was also observed that the resistance did not change appreciably for any of the specimens between the 255 cycle and the 760 cycle measurements. The greatest change was observed in the Gap Pad B samples, which decreased by 17 mm^2 K/W (25%), followed by the silicone putty, which experienced a change of about 9% on average. The observed reduction in thermal resistance may have been caused by the release of silicone from the TIM to the contacting surfaces, reducing the contact resistances by filling in the interstices. The gradual release of silicone oil, referred to as silicone extraction, is known to affect silicone elastomeric pads and can contaminate nearby components [27]. The gap filler samples showed a slight decrease of 1 mm^2K/W (1%) while the Gap Pad A samples, which contained no silicone, showed a slight increase of 12 mm^2K/W in resistance (5%), but in both cases the changes were within the uncertainty of the measurement. Higher levels of noise were observed in the temperature rise signals for the gap filler pads, which may have affected the accuracy of the measured 3-layer thermal diffusivity value. The standard deviation for the samples ranged between 5 mm^2K/W for the low resistance samples to 51 mm^2K/W for the high resistance samples. A comparison of the thermal resistance values throughout temperature cycling with the values from the room temperature study show that the changes in thermal resistance throughout the temperature cycling tests can be partly attributed to non temperature-related effects. The Gap Pad B samples, for instance, showed an 18% decrease after 30 days in the room temperature performance tests. The elevated temperature of the cycling tests may have accelerated the process occurring at room temperature.

Changes in Epoxy Adhesive Thermal Resistance

The adhesive TIMs subjected to temperature cycles decreased in thermal resistance initially, then gradually increased. Unlike the gap fillers and gap pads in this study, the adhesive was a dispensed epoxy material requiring a high temperature cure, so the resistance change could have been

caused by additional crosslinking after the samples were subjected to the high temperature cure. This general trend was observed in the samples used in the room temperature study as well. Of all the materials tested, the adhesive baseline resistance was dramatically lower than the room temperature tests, starting with the 10 minute value. In addition the adhesive experienced an enormous drop at room temperature but not in cycling. This may have been caused by differences in the application of the material as well as the effects of storage, as some samples contained adhesive in containers that had been thawed and then refrozen.

Observed Changes in Physical Appearance

While few changes were evident in the appearance of the TIM samples after temperature cycling, the Gap Pad A samples did show slight discoloration and increased stiffness after 255 and 510 cycles, most likely due to crosslinking of the polymer matrix. The thermal putty samples showed signs of "pump out" after 255 cycles. Figure 3 shows one sample after the first thermal performance measurement. The "before" image shown is for a different sample assembled in the same manner.

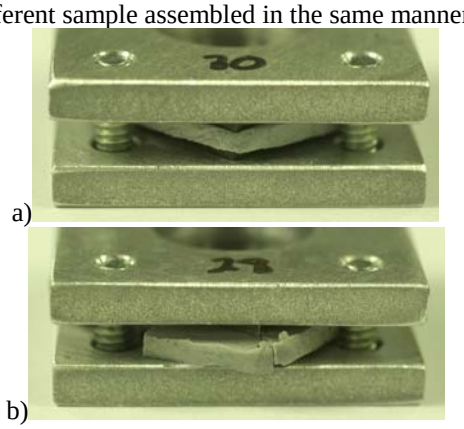

Figure 3: "Pump out" in the Thermal Putty Samples: a) Before Temperature Cycling; b) After 255 Temperature Cycling

This "pump out" was likely caused by the repeated expansion and contraction of the TIM relative to the sample holder structure during temperature cycling. Due to the concern over "pump-out," the thickness of this TIM type was measured prior to each intermediate thermal performance measurement and not assumed constant, as for the other samples. The thickness of the TIM layer was found to decrease an average of 0.1 mm as measured during each periodic thermal performance measurement. The screws were not tightened further after assembly. The excess material that was pumped out was removed to allow the TIM sample to fit in the sample holder during the laser flash measurement. Despite the "pump out" seen after only the first thermal performance measurement in the thermal putty samples, the putty experienced a reduction in part due to the thickness decrease.

Comparison with Vendor Values

Table 4 also shows the predicted thermal resistance values based on vendor thermal conductivity values and the average thickness of the samples during the baseline measurement. Except for the adhesive samples, the measured thermal resistance values were lower than those calculated using vendor thermal conductivity values. Since the objective of the study was to measure changes in thermal resistance throughout the temperature cycle tests, no attempt was made to ensure that the loading conditions in the test (particularly with regard to contact pressure) matched those used by vendors, which typically follow ASTM D5470 [1] or a modified form.

Uncertainty Analysis

Since the thermal resistance values are derived, errors can propagate through both the laser flash measurement and the uncertainty in the value of material properties needed for the calculations. The uncertainty in the TIM layer thermal resistance values used in this study was quantified by estimating the experimental accuracy of each measurement and determining the sensitivity of the TIM resistance to inputs in the Lee algorithm as summarized in Table 6. The thermal diffusivity of the 3-layer sandwich is assumed to be the same for the determination of each sensitivity term, leading to a conservative error estimate since changes in the inputs would lead to a change in the three-layer thermal diffusivity. The uncertainty value was determined to be on the order of 25 % based on an uncertainty of 31 mm^2K/W using representative values for a gap filler with a 123 mm^2K/W thermal resistance. The largest contributors to the uncertainty of the TIM layer resistance value appear to be the single layer density values and the 3-layer thermal diffusivity.

Table 5: Uncertainty Analysis Results

	Thickness			Density			Specific heat			Thermal diffusivity		
Layer	1	2	3	1	2	3	1	2	3	1	3	1+2+3
Error (%)	2.5	3.1	2.5	3.7	3.7	3.7	7	7	7	5	5	5
ΔR (mm^2K/W)	6.8	7.7	1.8	17.7	13.2	12.3	3.4	3.05	2.8	<0.1	3.5	13.0

Scanning Acoustic Microscope

Widely used in industry to detect defects and failures in IC components, scanning acoustic microscopy (SAM) was used in this study to detect voids and delamination and/or morphological changes that might explain changes in the thermal characteristics of the TIMs. This method can be useful given that the uncertainty in the calculated values based on laser flash measurements may not allow small changes in the thermal resistance to be detected with statistical confidence. Furthermore, because of the nature of the laser flash measurement, in which a thermal wave propagation through a sample material causes a temperature rise, the laser flash measurement may not capture all occurrences of delamination or voiding, particularly if the delamination regions are located

near the edges of where the laser beam area is incident on the sample.

To verify the viability of the technique, a gap filler specimen was prepared with a 0.5 mm thick spacer to induce a non-filled region between the copper and alloy 42 coupons. The non-filled region is clearly observed in the SAM image (shown in Figure 4).

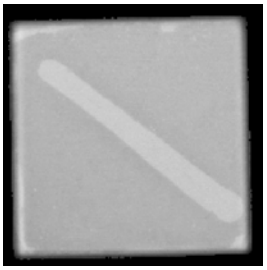

Figure 4: SAM Image of Gap Filler With Induced Delamination

Since the application of SAM requires that specimens be immersed in a liquid, SAM images were taken of a separate group of test samples that were assembled in the same manner as those used in the temperature cycling tests. This step prevented direct comparison of before and after temperature cycling images, but eliminated the influence of absorbed moisture affecting the thermal diffusivity measurements.

All measurements used a 75 MHz transducer and images were taken in C-scan mode. Only the sample area within the beam area was visible as the regions covered by the aluminum sample holder attenuated the acoustic signal, preventing those regions from being imaged. A pulse echo beam was used as this was suitable for the material combinations examined in the measurement.

The SAM measurements revealed delamination near the edges of the viewable area occurring at the TIM-copper coupon interfaces in nearly all of the Gap Pad A samples. A representative image is shown in Figure 5. A SAM image of a non-temperature cycled sample aged at room temperature and assembled at the same time as the temperature cycled one is shown for comparison in Figures 5, 6, and 7.

a) 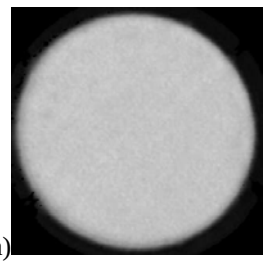 b) 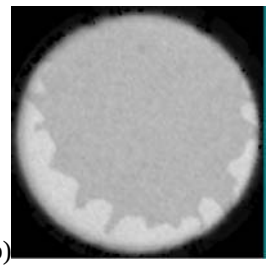

Figure 5: a) Non-Temperature Cycled Gap Pad A Sample
b) Temperature Cycled Gap Pad A Sample (after 760 cycles)

Cracking of the TIM layer in the temperature cycled putty samples was visible at the TIM-alloy 42 coupon interface, as shown in Figure 6. The dark spots were attributed to scratches on the graphite coating.

a) 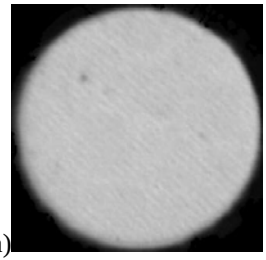 b) 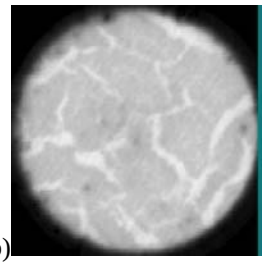

Figure 6: a) Non-Temperature Cycled Putty Sample
b) Temperature Cycled Putty Sample (after 760 cycles)

Regions of nonuniform TIM coverage were visible in all of the SAM images of the temperature cycled adhesive samples, as shown in Figure 7. This may have resulted from how the adhesive was dispensed onto the coupons as well as additional crosslinking of the epoxy adhesive during temperature cycling. SAM measurements did not reveal any loss of contact at the TIM-coupon interfaces for the Gap Pad B and gap filler samples.

a) 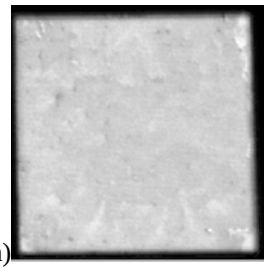 b) 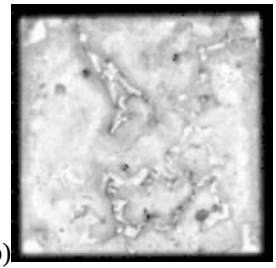

Figure 7: a) Non-Temperature Cycled Adhesive Sample
b) Temperature Cycled Adhesive Sample (after 760 cycles)

CONCLUSIONS

Little change or a reduction in thermal resistance was observed throughout temperature cycling for the samples in this study. Gap Pad A experienced a six percent resistance increase that was within the experimental uncertainty and showed delamination occurring at the TIM-copper coupon interfaces. Gap Pad B experienced the greatest thermal resistance reduction throughout temperature cycling followed by the putty, the adhesive, and the gap filler. One effect of the temperature cycling on the putty samples was expansion of the TIM layer, leading to cracks that were visible in the SAM images. Silicone extraction may have helped reduce the contact resistance of the silicone-based TIMs in this study although additional crosslinking may have been the primary reason for

the improvement in thermal performance of the epoxy adhesive.

Under room temperature aging, a gradual reduction in thermal resistance was measured for all TIMs between the initial assembly and 30 days after assembly, which indicated that the thermal resistance reduction during temperature cycling may not have been only a temperature-related effect. SAM images did not reveal any loss of contact at the TIM-coupon interfaces in either the as-prepared test specimens or the temperature-cycled test specimens of the Gap Pad B and gap filler. However, regions of nonuniform coverage were visible in SAM images of the temperature-cycled adhesive samples.

A conservative estimate of the TIM layer thermal resistance of about 25% suggests that inaccuracy in the single layer input values and measured 3-layer diffusivity values can dramatically affect the TIM resistance values. The results of the temperature cycling tests performed in this study suggest that the selected TIMs perform reliably in temperature cycling conditions.

Although the goal of the experimental procedure was to develop a method to measure changes in thermal resistance, the thermal resistance values of the non-adhesive TIMs were found to be lower than those calculated from the effective conductivity values reported by vendors, which typically used the ASTM D5470 standard or a modified form. These results may have been caused by differences in the contact pressure, which could have affected both contact and bulk resistances, or nonuniform surface heating of the test samples during the laser flash measurement.

REFERENCES

[1] Nakayama, W., and Bergles, A., "Thermal Interfacing Techniques for Electronic Equipment-A Perspective," *Journal of Electronic Packaging*, Vol. 125, 2003, pp. 192-199.

[2] Lasance, C., "The Urgent Need for Widely Accepted Test Methods for Thermal Interface Materials," *Proceedings of SEMITHERM XIX*, March 2003, San Jose, pp. 123-128.

[3] Dean, N.F. and A.L. Gettings, "Experimental Testing of Thermal Interface Materials on Non-Planar surfaces", *Proceedings of SEMITHERM XIII*, San Diego , CA, 1998, pp. 88-94.

[4] Test Method D5470-01, "Standard Test Method for Thermal Transmission Properties of Thin, Thermally Conductive Solid Electrical Insulation Materials," American Society for Testing and Materials, 2001.

[5] Test Method E1461-01, "Standard Test Method for Thermal Diffusivity of Solids by the Flash Method," American Society for Testing and Materials, Annual Book of ASTM Standards, Vol. 14.02, 2001.

[6] Gwinn, J., Saini, M., Webb, R., "Apparatus for Accurate Measurement of Interface Resistance of High Performance Thermal Interface Materials," *Proceedings ITHERM 2002*, pp. 644-650.

[7] Culham, J., Teerstra, O., Savija, I., Yovanovich, M., "Design, Assembly and Commissioning of a Test Apparatus for Characterizing Thermal Interface Materials," *Proceedings ITHERM 2002*, San Diego, California, USA, May 30-June 1, 2002, pp. 128-134.

[8] Samson, E.C., Machiroutu, S.V., Chang, J.Y., Santos, I., Hermerding., J., Dani, A., Prasher, R., Song, D.W., "Interface Material Selection and a Thermal Management Technique in Second-Generation Platforms Built on Intel Centrino Mobile Technology," *Intel Technology Journal*. Vol. 9, Issue 1, Feb. 17, 2005.

[9] Chiu, C.-P, Chandran, B., Mello, M., Kelley, K., "An Accelerated Reliability Test Method to Predict Thermal Grease Pump-Out in Flip-Chip Applications," *Proceedings of 51th Electronic Components & Technology Conference*, Orlando, FL, May/June 2001, pp. 91-97.

[10] Gowda, A., Zhong, A., Esler, D., David, J., Tonapi, S.S., Schattenmann, F., and Srihari, K., "In-Situ Performance of Silicone Thermal Interface Materials: Influence of Filler Characteristics," *Proceedings of Polytronic 2003*, Switzerland, October 2003, pp. 177-182.

[11] Matayabas, J.C., and LeBonheur, V., "Silicone Gel Thermal Interface Materials for High Heat Dissipation and Thermo-Mechanical Stress Management for Good Reliability Performance," *Proceedings of I-pack 2005*, July 17-22, San Francisco, CA, pp. 1863-1873.

[12] Eveloy, V., Rodgers, P. and Pecht, M., 2004, "Reliability of Pressure-Sensitive Adhesive Tapes for Heat Sink Attachment in Air-Cooled Electronic Assemblies," *IEEE Transactions on Device and Materials Reliability*, Vol. 4, No. 4, pp. 650-657.

[13] Gowda, A., Esler, D., Paisner, S., Tonapi, S., Nagarkar, K., "Reliability Testing of Silicone-Based Thermal Grease," *Proceedings of SEMITHERM XXI*, San Jose, California, March 2005. pp. 64-71.

[14] Chiu, C.-P., Maveety, J.G., and Tran, Q.A., "Characterization of Solder Interfaces Using Laser Flash Metrology," *Microelectronics Reliability*, January 2002, Vol. 42, Iss. 1, pp. 93-100.

[15] Campbell, R.C., Smith, S.E., and Dietz, R.L., "Measurements of Adhesive Bondline Effective Thermal Conductivity and Thermal Resistance Using the Laser Flash Method", *Proceedings of SEMITHERM XV*, 1999, pp. 83-97.

[16] Maguire, L, Behnia, M. and Morrison, G., "Systematic Evaluation of Thermal Interface Materials – a Case Study in High Power Amplifier Design," *Microelectronics Reliability*, Vol. 45, 2005, pp. 711-725.

[17] Viswanath, R., Wakharkar, V., Watwe, A., Lebonheur, V., "Thermal Performance Challenges from Silicon to Systems," *Intel Technology Journal*. Vol. Issue 2, May 16, 2002.

[18] Parker, W., Jenkins, R., Butler, C., and Abbott, G., "Flash Method of Determining Thermal Diffusivity, Heat Capacity, and Thermal Conductivity," *Journal of Applied Physics*, Vol. 32, No. 9, Sept. 1961. pp. 1679-1684.

[19] Cowan, R. D., "Pulse Method of Measuring Thermal Diffusivity at High Temperatures," *Journal of Applied Physics*, Vol. 34, Issue 4, Part 1, 1963, pp. 926 - 927.

[20] Clark, L. M. and Taylor, R. E., "Radiation Loss in the Flash Method for Thermal Diffusivity." *Journal of Applied Physics*, Vol. 46, Issue 2, 1975, pp. 714-719.

[21] Koski, J. A., "Improved Data-Reduction Methods for Laser Pulse-Diffusivity Determination with the Use of Minicomputers," *Intern. Joint Conf. on Thermophys. Properties*, Gaithersburg, Md., 15 Jun. 1981, pp 94-103.

[22] Dasgupta, A., "Thermomechanical Analysis and Design," *Handbook of Electronic Package Design*, Ed. Michael Pecht, M., Marcel Dekker, Inc., 1991.

[23] Lee, H.J., Purdue University Ph.D. Thesis, "Thermal Diffusivity in Layered and Dispersed Composites," University Microfilms International, 1975.

[24] Lee, T.R., Purdue University Ph.D. Thesis, "Thermal Diffusivity of Dispersed and Layered Composites," University Microfilms International, 1977.

[25] Graebner, J., "Measuring Thermal Conductivity and Diffusivity," *Thermal Measurements in Electronics Cooling*, Ed. Azar, K., Boca Raton, FL: CRC Press LLC, 1997.

[26] IPC Standard IPC SM-785, "Standard Test Method for Surface Mount Solder Attachments," Lincolnwood, IL, January 1995.

[27] Application Note 056: Note on Gap Pad Silicone Extraction. The Bergquist Company, http://www.bergquistcompany.com/objects/Technical_Library/Application_Notes/APN_056.pdf, Retrieved 2/13/07.